Available online at www.sciencedirect.com
SCIENCE DIRECT®
Journal of Nuclear Materials 344 (2005) 67–72
journal of nuclear materials
www.elsevier.com/locate/jnucmat

Phase equilibria and thermal expansion of $CaTiO_3$ doped with neptunium

Tsuyoshi Sato [a], Toshiyuki Yamashita [b,*], Tsuneo Matsui [a]

[a] *Department of Quantum Engineering, Graduate School of Engineering, Nagoya University, Furo-cho, Chikusa-ku, Nagoya 464-8603, Japan*
[b] *Advanced Science Research Center, Japan Atomic Energy Research Institute, Tokai, Ibaraki 319-1195, Japan*

Abstract

Phase relationships between NpO_2 and $CaTiO_3$ or $Ca(Ti,Al)O_3$ were investigated by X-ray diffraction (XRD) analysis at room temperature, using specimens prepared at 1773 K in Ar–8%H_2 atmosphere. Single phase solid solutions were formed for 0–7.5 mol% Np doped $CaTiO_3$ and 1–10 mol% Np doped $Ca(Ti,Al)O_3$. By substituting Al for Ti in $CaTiO_3$, Np solubility in $Ca(Ti,Al)O_3$ increased. Thermal expansions of $(Ca_{1-x}Np_x)TiO_3$ ($x = 0.03$, 0.05 and 0.075) were measured for temperatures between room temperature and 1273 K in Ar-8%H_2 atmosphere using high-temperature XRD technique. Volumetric thermal expansion coefficients of these three specimens were nearly the same value, suggesting that the incorporation of tetravalent Np into $CaTiO_3$ had practically no effect on stabilization of the crystal lattice.

1. Introduction

Ceramic waste forms of natural analogues are promising candidates for the high-level waste (HLW) disposal especially for long half-life transuranium (TRU) elements, because of their high thermodynamic stability for a long time [1]. The perovskite ($CaTiO_3$) type phase is one of the major phases of SYNROC (SYNthetic ROCk), a titanate ceramic waste form which is a potential matrix for immobilizing high-level nuclear waste. It is thus of importance to study the phase equilibria of $CaTiO_3$ containing TRU elements from the viewpoint of not only practical use as a ceramic waste form but also basic research on the crystal chemistry, because TRU elements may change the oxidation state depending on heating conditions.

Phase equilibria of $CaTiO_3$ doped with Ce, U and Pu have been studied by X-ray diffraction (XRD) [2,3], where Ce and U were surrogates for TRU elements. Solubility of Ce and U in $CaTiO_3$ prepared at 1600 K in purified argon ($P_{O_2} \sim 10^{-10}$ Pa) were 20–30 mol% and below 3 mol%, respectively. X-ray absorption fine structure (XAFS) analysis [4] revealed that part of the tetravalent Ce in $CaTiO_3$ prepared in purified argon was reduced to trivalent, while the oxidation state of U in $CaTiO_3$ was remained tetravalent under the same conditions. Plutonium was soluble in $CaTiO_3$ up to at

* Corresponding author. Tel.: +81 29 282 5416; fax: +81 29 282 5927.
E-mail address: yamasita@popsvr.tokai.jaeri.go.jp (T. Yamashita).

0022-3115/$ - see front matter © 2005 Elsevier B.V. All rights reserved.
doi:10.1016/j.jnucmat.2005.04.018

least 20 mol% at 1673 K in Ar–8%H_2 ($P_{O_2} \sim 10^{-17}$ Pa), but Pu solubility in $CaTiO_3$ prepared in air and in vacuum was extremely limited (<5 mol%). Under oxidizing conditions the oxidation state of Pu is considered to be tetravalent. The limited solubility of tetravalent dopants is ascribed to difference in oxidation state compared with that of host Ca^{2+} ion.

Excess charges which are introduced by incorporation of trivalent/tetravalent cations can be compensated by Al substitution for Ti and hence solubility of these cations may increase by this approach. Uranium solubility in $Ca(Ti,Al)O_3$ was 5–7.5 mol% at 1600 K in purified argon [2]. By substituting Al for Ti in $CaTiO_3$, tetravalent uranium solubility seemed to increase. Begg et al. [5] reported that tetravalent Pu and Np solubility in perovskite increased to 14 and 16 mol%, respectively, by substituting Al for Ti.

For this study the phase relationships between NpO_2 and $CaTiO_3$ or $Ca(Ti,Al)_3$ have been investigated by XRD. Thermal expansions of some single phase $(Ca_{1-x}Np_x)TiO_3$ ($x = 0.03$, 0.05 and 0.075) solid solutions were also measured by high-temperature XRD.

2. Experimental

2.1. Materials

Starting materials were $CaCO_3$, TiO_2 and Al_2O_3 powders of 99.99% purity supplied by Rare Metallic Co., Tokyo, and the 99.8% pure $^{237}NpO_2$ powder (0.2% $^{238}Pu + {}^{241}Am$ as impurities) supplied by AEA Technology, UK. Sample compositions were $(Ca_{1-x}Np_x)TiO_3$ ($x = 0.03$, 0.05, 0.075 and 0.10) and $(Ca_{1-x}Np_x)(Ti_{1-2x}Al_{2x})O_3$ ($x = 0.03$, 0.05, 0.075, 0.10 and 0.15). In the former case the charge balance was supposed to be maintained by reduction of Ti^{4+} to Ti^{3+} [6–8]. In the latter case Al^{3+} was added twice as much as the amount of Np^{4+} to compensate for the excess charge. The Al dopant was supposed to substitute for Ti^{4+}.

Starting material powders were weighed and mixed, and then calcined at 1273 K for 6 h in air. After pressing into pellets, they were heated at 1773 K for 6 h in Ar–8%H_2 and then pulverized in an agate mortar. Heating and pulverizing processes were repeated several times until the formation reaction was completed. Products were analyzed by XRD every time after heating. Some specimens with nominal composition of $(Ca_{1-x}Np_x)TiO_3$ ($x = 0.05$ and 0.075) and $(Ca_{1-x}Np_x)(Ti_{1-2x}Al_{2x})O_3$ ($x = 0.05$, 0.075 and 0.10) were annealed at 1273 K in air to investigate phase relationships in oxidizing conditions.

2.2. X-ray diffraction study

Powder XRD patterns were taken at room temperature or at elevated temperature using a Rigaku RAD-3C diffractometer system equipped with a furnace unit. A vacuum housing and a Pt heating element enabled to carry out measurements in a controlled atmosphere of He–8%H_2 gas at high temperature. Furnace temperature was measured by an R-type thermocouple inserted into a thin hole of a sample holder and was controlled within ±1 K during the measurements. CuKα radiation was monochromatized with curved pyrolytic graphite.

Before X-ray measurements, each specimen was heated at 1273 K for 1 h in He–8%H_2. The furnace temperature was then decreased by 50 K or 100 K and kept constant for 1 h, and the X-ray measurements were carried out. A detailed description of the high-temperature XRD method has been given in a previous paper [9].

XRD patterns were recorded in the range from $2\theta = 20°$ to 80°. Due to the low symmetry of $CaTiO_3$, Pbnm, peaks at high diffraction angles were weak and broad. Lattice parameters were calculated using reflections in the range of $20° < 2\theta < 80°$ employing the least-squares method for the Nelson–Riley extrapolation [10]. Estimated standard errors of the calculated lattice parameters were less than ±0.0002 nm.

3. Results

3.1. Incorporation of neptunium

Although all the observed peaks could be indexed by the orthorhombic space group Pbnm, the overlapped intensity from (1 1 0) and (0 0 2) planes shows an irregular variation with Np content as shown in Fig. 1. The upper one is for $(Ca_{1-x}Np_x)TiO_3$ ($x = 0$–0.10) and the lower for $(Ca_{1-x}Np_x)(Ti_{1-2x}Al_{2x})O_3$ ($x = 0$–0.15). Atom arrangements in the $CaTiO_3$ lattice can be obtained by analyzing such intensity variations. Intensity calculations were performed by using the X-ray intensity expression [11] and crystallographic data [12] for two possible atom arrangements: (1) Np dopant substituted for Ca and (2) Np dopant substitute for Ti. Fig. 2 shows calculated intensities of the overlapped peak from (1 1 0 and 0 0 2) planes together with the observed ones, where calculated intensities are normalized against the observed one for pure $CaTiO_3$. Observed and calculated intensities are indicated by open and closed marks, respectively. For both $(Ca_{1-x}Np_x)TiO_3$ and $(Ca_{1-x}Np_x)(Ti_{1-2x}Al_{2x})O_3$ system, calculated intensities assuming case 1 arrangement well represented the observed intensity changes. On the other hand, in the case 2 arrangement, calculations yielded intensities which were completely the opposite of the observed ones.

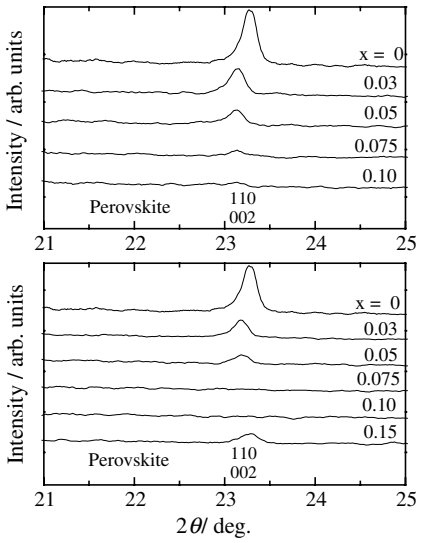

Fig. 1. Intensity variation of the X-ray diffraction peaks of $hkl = (110$ and $002)$ for $(Ca_{1-x}Np_x)TiO_3$ (upper part) and $(Ca_{1-x}Np_x)(Ti_{1-2x}Al_{2x})O_3$ (lower part).

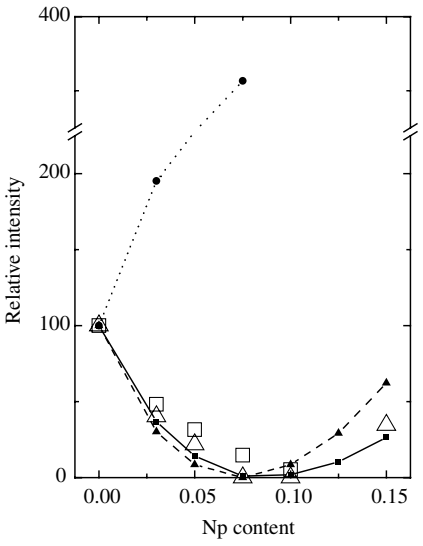

Fig. 2. Comparison of compositional dependence between the calculated intensities of $hkl = (110$ and $002)$ and the observed ones. Open marks are the observed values. □: $(Ca,Np)TiO_3$, $hkl = (110$ and $002)$; △: $(Ca,Np)(Ti,Al)O_3$, $hkl = (110$ and $002)$. Closed marks are the calculated values. ■: $(Ca,Np)TiO_3$, Np on Ca site, $hkl = (110$ and $002)$; ▲: $(Ca,Np)(Ti,Al)O_3$, Np on Ca site, $hkl = (110$ and $002)$; ●: $Ca(Ti,Np)TiO_3$, Np on Ti site, $hkl = (110$ and $002)$.

These simulation calculations clearly showed that the dopant Np mainly substitutes for Ca in the $CaTiO_3$ lattice.

3.2. Phase equilibria

Lattice parameters and cell volumes of $(Ca,Np)TiO_3$ and $(Ca,Np)(Ti,Al)_3$ samples prepared at 1773 K in Ar–8%H_2 are shown as a function of Np content in Fig. 3(a) and (b), respectively. In these figures lattice parameters are plotted as $a/\sqrt{2}$, $b/\sqrt{2}$ and $c/2$. The lattice parameter of the orthorhombic Pbnm perovskite structure, a, b and c, can be expressed as $a \cong \sqrt{2}a_{ideal}$, $b \cong \sqrt{2}a_{ideal}$ and $c \cong 2a_{ideal}$ using the lattice parameter of the ideal cubic perovskite structure, a_{ideal}. As can be seen from the Fig. 3(a) lattice parameters a, b, and c, and cell volume increase linearly with increasing Np content up to 7.5 mol% ($x = 0.075$), and then deviate from the linearity. Unreacted NpO_2 residue, which was frequently detected in the course of sample preparation, was not identified in the XRD pattern of $x = 0.075$ sample but was identified in that of $x = 0.10$ sample. It is therefore concluded that up to 7.5–10 mol% Np can be incorporated in $CaTiO_3$ at 1773 K under reducing atmosphere of Ar–8%H_2 ($P_{O_2} \sim 10^{-17}$ Pa).

Lattice parameters of $(Ca,Np)(Ti,Al)_3$ samples do apparently not vary monotonously with Np content as seen in Fig. 3(b). The cell volume, on the other hand, decreases linearly with Np content up to $x = 0.10$ and then at $x = 0.15$ deviates from the regression line. Residual NpO_2 was also recognized in the XRD pattern of $x = 0.15$ sample, suggesting that Np solubility in $Ca(Ti,Al)O_3$ amounts 10–15 mol% at 1773 K under reducing conditions. Apparently Np solubility may be enhanced by substituting Al for a part of Ti in $CaTiO_3$, as has been demonstrated for U-doped $CaTiO_3$ [2].

In order to investigate the phase relations of $(Ca_xNp_{1-x})TiO_3$ and $(Ca_xNp_{1-x})(Ti_{1-2x}Al_{2x})O_3$ in oxidizing conditions, these samples prepared in Ar–8%H_2 atmosphere at 1773 K were annealed in air at 1273 K for 6 h. All samples of $(Ca_xNp_{1-x})TiO_3$ were converted into two phase mixture of NpO_2 and perovskite-type phase. Under oxidizing condition the Np solubility in $CaTiO_3$ was extremely limited as in the cases of the U-doped [2] and the Pu-doped samples [3]. On the other hand, $(Ca_xNp_{1-x})(Ti_{1-2x}Al_{2x})O_3$ samples were perovskite-type single phase except for $(Ca_{0.95}Np_{0.05})(Ti_{0.90}Al_{0.10})O_3$ where a trace amount of NpO_2 was identified as a second phase. Lattice parameters, a, b and c, and cell volume of $(Ca_xNp_{1-x})(Ti_{1-2x}Al_{2x})O_3$ decreased linearly with increasing Np content up to 10 mol%. These results showed that the addition of trivalent Al was very effective to increase the solubility of tetravalent Np in $CaTiO_3$ especially under oxidizing condition where Ti^{4+} could not be reduced easily to Ti^{3+}.

3.3. Thermal expansion

Fig. 4 shows the typical variation of lattice parameters and cell volume of $(Ca_{0.95}Np_{0.05})TiO_3$ with

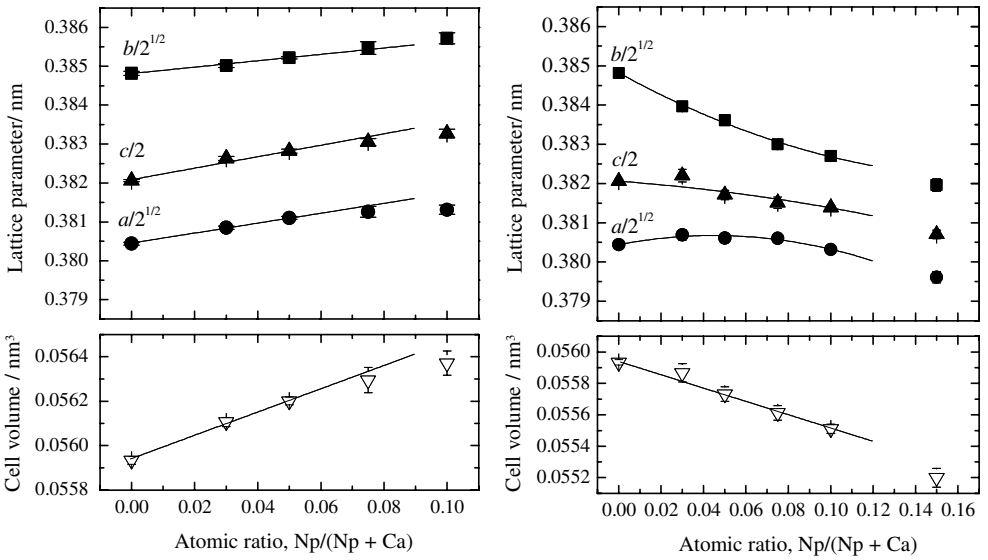

Fig. 3. Compositional dependence of lattice parameters and cell volume of $(Ca_{1-x}Np_x)TiO_3$ (a) and $(Ca_{1-x}Np_x)(Ti_{1-2x}Al_{2x})O_3$ (b) at room temperature. Samples were prepared in Ar–8%H_2. Lattice parameters at $x = 0.00$ were those from our previous study [4]. ●: $a/\sqrt{2}$; ■: $b/\sqrt{2}$; ▲: $c/2$; ▽: cell volume; —: regression line.

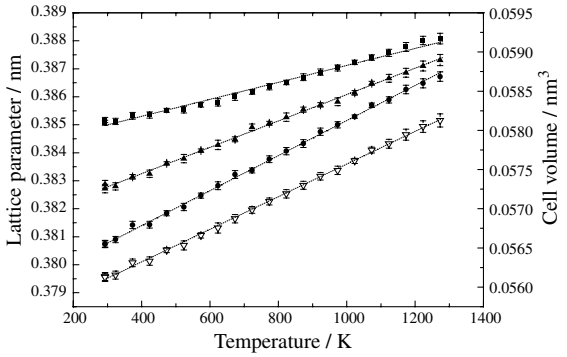

Fig. 4. Temperature dependence of lattice parameters of $(Ca_{0.95}Np_{0.05})TiO_3$ prepared in He–8%H_2. Cell volume $(V) = a/\sqrt{2} \times b/\sqrt{2} \times c/2 = abc/4$. ●: $a/\sqrt{2}$; ■: $b/\sqrt{2}$; ▲: $c/2$; ▽: cell volume; ···: regression line.

temperature measured in He–8%H_2. All lattice parameters and cell volume are seen to increase smoothly with increasing temperature up to about 1300 K. Measured lattice parameters were fitted as a function of temperature: $a(T)/\sqrt{2} = A_0 + A_1T$, $b(T)/\sqrt{2} = B_0 + B_1T$ and $c(T)/2 = C_0 + C_1T$. The regression results are listed in Table 1. Linear thermal expansion coefficients of *a*-, *b*- and *c*-axes and a volumetric thermal expansion coefficient were calculated using values given in Table 1, and are summarized in Table 2. The $(Ca_{1-x}Np_x)TiO_3$ samples show a considerable anisotropic thermal expansion like pure $CaTiO_3$ [13–15] and Pu-doped $CaTiO_3$ [3]. Calculated linear thermal expansion coefficients, α_a, α_b, and α_c, for orthorhombic Pbnm structure are in the order $\alpha_a > \alpha_c > \alpha_b$, which is the same result as those reported previously.

Table 1
Regression data of lattice parameter expansions for $(Ca_{1-x}Np_x)TiO_3$

x	A_0	10^6A_1	B_0	10^6B_1	C_0	10^6C_1
0.03	0.3790	5.8879	0.3838	2.9230	0.3809	4.8639
0.05	0.3789	6.2607	0.3841	3.0310	0.3814	4.7085
0.075	0.3793	6.1749	0.3844	2.7885	0.3816	4.7840

$a(T)/\sqrt{2} = A_0 + A_1T$, $b(T)/\sqrt{2} = B_0 + B_1T$, $c(T)/2 = C_0 + C_1T$.

Table 2
Thermal expansion coefficients (10^6 K^{-1}) of $(Ca_{1-x}Np_x)TiO_3$

x	Temp. range (K)	α_a	α_b	α_c	α_V
0.03	298–1273	15.9 ± 0.4	7.97 ± 0.4	12.8 ± 0.3	36.7 ± 0.8
0.05	298–1273	16.4 ± 0.2	7.87 ± 0.2	12.3 ± 0.2	36.6 ± 0.8
0.075	298–1273	16.2 ± 0.2	7.24 ± 0.2	12.5 ± 0.2	36.0 ± 0.7

4. Discussion

The solubility of Np in $CaTiO_3$ in Ar–8%H_2 mixed gas flow is smaller than that of Pu in $CaTiO_3$: 7.5–10 mol% for Np and at least 20 mol% for Pu [3]. Oxidation states and ionic radii of dopant cations seem to have significant influence on their solubility in $CaTiO_3$. The

oxidation state of Np in $CaTiO_3$ is not known yet. However, Np^{4+} reduction to Np^{3+} was never observed in our previous studies on the U–Np–O system [16,17] nor Np-doped $(Zr,Y)O_{2-x}$ solid solution [18] under reducing conditions. Therefore the oxidation state of Np in $(Ca,Np)TiO_3$ is considered to be almost tetravalent. The ionic radius of Np^{4+} with CN = 12 is expected to be 0.116 nm which is estimated from the U^{4+} ionic radius of 0.117 nm [19]. No data are available about the exact oxidation state of Pu in $(Ca,Pu)TiO_3$ samples and ionic radii of Pu^{3+} and Pu^{4+} with 12 coordination number (CN). It seems reasonable to assume that these properties of Pu are similar to those of Ce in $(Ca,Ce)TiO_3$, because of the similarity in chemical behavior and the fact that Pu solubility in $CaTiO_3$ was nearly the same as that of Ce in $CaTiO_3$. Hanajri et al. estimated that the Ce oxidation state was 3.2 by analyzing the X-ray absorption near edge structure (XANES) spectrum of Ce-L_{III} edge [20]. As the ionic radii of Ce^{4+} and Ce^{3+} with CN = 12 are 0.114 nm and 0.134 nm [19], respectively, the mean ionic radius of Ce in the $(Ca,Ce)TiO_3$ sample prepared in reducing condition is calculated to be 0.130 nm, which is comparable to that of Ca^{2+}, 0.134 nm [19]. Differences in both oxidation state and ionic radii between host Ca and Np are larger than those between host Ca and Pu. Therefore the solubility of actinide dopants in $CaTiO_3$ is thought to be governed mainly by the oxidation state and the corresponding mean ionic radius of dopants in reference to those of host Ca^{2+}.

The thermal expansion coefficient, α_L, can be connected with the melting temperature of the compound through $\alpha_L\ (M_p - 273.15) = \text{constant}$, where M_p is the melting temperature in K. As pointed out by Uitert et al. [21], these values are taken as a direct measure of binding energy. Since the $(Ca_{1-x}M_x)TiO_3$ (M = Pu and Np) showed anisotropic thermal expansions, the average thermal expansion coefficient was assumed to be equal to a third of the volumetric thermal expansion coefficient. Measured values of the volumetric thermal expansion for $(Ca_{1-x}Np_x)TiO_3$ are almost similar for all compositions within the experimental errors as seen in Table 2. The value of about $(36 \pm 1) \times 10^{-6}\ K^{-1}$ is also the same as that of pure $CaTiO_3$ [3]. These facts suggest that the incorporation of Np into $CaTiO_3$ has no effect on the stability of the crystal lattice. This was in a marked contrast to that of Pu doped $CaTiO_3$, where pronounced stabilization in the crystal was observed by incorporation of Pu into $CaTiO_3$ [3].

5. Conclusion

Analyses on variation of XRD peak intensities with Np contents suggested that the doped Np substituted for Ca in the lattice. Neptunium solubility was found to be 7.5–10 mol% and 10–15 mol% in $CaTiO_3$ and in $Ca(Ti,Al)O_3$, respectively. Aluminum substitution for Ti in $CaTiO_3$ was very effective to increase Np solubility. Under oxidizing conditions an extremely limited amount of Np was incorporated in $CaTiO_3$. Solubility in $CaTiO_3$ was thought to be influenced mainly by the oxidation state and the corresponding ionic radius of dopant cation in reference to those of host Ca^{2+}.

The $(Ca_{1-x}Np_x)TiO_3$ samples showed a considerable anisotropic thermal expansion in the order $\alpha_a > \alpha_c > \alpha_b$. Volumetric thermal expansion coefficients of these samples were about $(36 \pm 1) \times 10^{-6}\ K^{-1}$ and did not change with Np contents, indicating that the incorporation of Np into $CaTiO_3$ had no effect on stabilizing its crystal lattice.

Acknowledgments

The authors would like to thank Drs Ogawa and Minato of Japan Atomic Energy Research Institute for their encouragement and support to the present work. This work has been performed under the joint research project between Japan Atomic Energy Research Institute and Universities on Backend Chemistry.

References

[1] G.R. Lumpkin, K.L. Smith, M.G. Blackford, J. Nucl. Mater. 224 (1995) 31.
[2] Y. Hanajiri, H. Yokoi, T. Matsui, Y. Arita, T. Nagasaki, J. Nucl. Mater. 247 (1997) 285.
[3] T. Sato, Y. Hanajiri, T. Yamashita, T. Matsui, T. Nagasaki, J. Nucl. Mater. 294 (2001) 130.
[4] Y. Hanajiri, T. Matsui, Y. Arita, T. Nagasaki, H. Shigematsu, T. Harami, Solid State Ionics 108 (1998) 343.
[5] B.D. Begg, E.R. Vance, S.D. Conradson, J. Alloys Comp. 271–273 (1998) 221.
[6] Hj. Matzke, I.L.F. Ray, B.W. Seatonberry, H. Thiele, C. Trisoglio, C.T. Walker, T.J. White, J. Am. Ceram. Soc. 73 (1990) 370.
[7] W.J. Buykx, K. Hawkins, D.M. Levins, H. Mitamura, R.St.C. Smart, G.T. Stevens, K.G. Watson, D. Weedon, T.J. White, J. Am. Ceram. Soc. 71 (1988) 678.
[8] C.J. Ball, W.J. Buykx, F.J. Dickson, K. Hawkins, D.M. Levins, R.St.C. Smart, K.L. Smith, G.T. Stevens, K.G. Watson, D. Weedon, T.J. White, J. Am. Ceram. Soc. 72 (1989) 404.
[9] T. Yamashita, N. Nitani, T. Tsuji, H. Inagaki, J. Nucl. Mater. 245 (1997) 72.
[10] J.B. Nelson, D.P. Riley, Proc. Phys. Soc. (London) 57 (1945) 160.
[11] B.D. Cullity, Elements of X-ray Diffraction, Addison-Wesley Publishing Company, Reading, Massachusetts, USA, 1956.
[12] International Tables for X-ray Crystallography, vol. III, Reidel, 1985, p. 201.

[13] C.J. Ball, G.J. Thorogood, E.R. Vance, J. Nucl. Mater. 190 (1992) 298.
[14] X. Liu, R.C. Liebermann, Phys. Chem. Miner. 20 (1993) 171.
[15] S.A.T. Redfern, J. Phys.: Condens. Matter 8 (1996) 8267.
[16] T. Yamashita, N. Nitani, K. Ohuchi, T. Muromura, T. Tsuji, H. Inagaki, T. Kato, J. Alloys Comp. 213/214 (1994) 375.
[17] T. Yamashita, N. Nitani, T. Tsuji, T. Kato, J. Nucl. Mater. 247 (1997) 90.
[18] T. Yamashita, K. Kuramoto, M. Nakada, S. Yamazaki, T. Sato, T. Matsui, J. Nucl. Sci. Technol. Suppl. 3 (2002) 585.
[19] R.D. Shannon, Acta Cryst. A 32 (1976) 751.
[20] Y. Hanajiri, Y. Arita, T. Matsui, Private communication.
[21] L.G. Van Uitert, H.M. O'Bryan, M.E. Lines, H.J. Guggenheim, G. Zydzik, Mater. Res. Bull. 12 (1977) 261.